INDONESIAN JOURNAL ON GEOSCIENCE
Geological Agency
Ministry of Energy and Mineral Resources

Journal homepage: http://ijog.geologi.esdm.go.id
ISSN 2355-9314, e-ISSN 2355-9306

Characterization of Reservoir Rocks of X Gas Field, Surma Basin, Bangladesh

*Afroza Parvin[1], Md. Jamilur Rahman[1], Abdus Samad[1], and A.S.M. Woobaidullah[2]

[1]Department of Geology, University of Dhaka, Dhaka-1000
[2]Professor, Department of Geology, University of Dhaka, Dhaka-1000

Corresponding author: ap13geo@gmail.com
Manuscript received: July, 23, 2018; revised: December, 16, 2019;
approved: April, 1, 2021; available online: September, 10, 2021

Abstract - This paper deals with the rock physical analysis of primary reservoir rocks in the X gas field, which includes identifying the transition zone between mechanical and chemical compaction zones and the amount of cement in the reservoir rock. The analysis is performed by plotting different log data (Gamma-ray, density, neutron porosity, and sonic log) against depth, constructing the cross plot, and plotting of sonic and porosity logs with cement model. The transition zone, which is the boundary between mechanical and chemical compactions, indicates a sharp increase in density and a decrease in porosity with no lithological change at 2,576 m depth (Well-2). Among three gas sands, the upper gas sand and upper part of the middle gas sand are located within the mechanical compaction zone. The lower parts of the middle gas sand and lower gas sand are within the chemical compaction zone. Cement model analysis showed that the upper gas sand and upper part of the middle gas are composed of unconsolidated sand. In contrast, the lower part of middle gas sand and lower gas sand comprise of consolidated sand, having almost 2% contact cement.

Keywords: rock physics, compaction processes, cement model, reservoir management

How to cite this article:
Parvin, A., Rahman, Md.J., Samad, A., and Woobaidullah, A.S.M., 2021. Characterization of Reservoir Rocks of X Gas Field, Surma Basin, Bangladesh. *Indonesian Journal on Geoscience*, 8 (3), p.417 - 426. DOI: 10.17014/ijog.8.3.417-426

Introduction

The Surma Basin is the Subbasin of Bengal Basin located in the NE part of Bangladesh, the central gas-rich province. Among the twenty-six gas fields discovered in Bangladesh, eighteen gas fields are located in the Surma Basin. The total recoverable proven and probable gas reserve of twenty-six gas fields have been estimated to be at 27.12 TCF, out of which 12.45 TCF was produced, leaving only 14.55 TCF (Petrobangla, 2015). The country gas demand has already surpassed about 3,200 million cubic feet per day, whereas the average supply of gas is around 2,700 MMCFD (Petrobangla Annual Report, 2016). The demand-supply mismatch has been a longstanding problem in the country energy sector. In this situation, sustainable management of the gas field is essential, along with discovering new gas fields. Therefore, proper reservoir characterization in any gas field is necessary to do the proper reservoir management. The reservoir properties, *i.e.* stiffness, porosity, permeability, ongoing diagenetic process *etc.* depend on the depositional and diagenetic process of a basin. When sediments were first deposited in the basin, they were in a liquid-like state, loose, porous, and unstable. Then these sediments underwent a series of changes with time, depth, and temperature. The most important change is the loss/

gradual decrease of porosity by mechanical and chemical compaction where mechanical compaction (MC) is stress-dependent, and chemical compaction (CC) depends on the temperature. Reservoir rock initially experiences mechanical compaction (MC) with depth, which ceases at a specific temperature when chemical compaction (CC) started. This process changes the reservoir rock properties, *i.e.* decreasing porosity and increasing velocity and density through progressive burial at greater depth. The zone with this specific temperature (about 69 - 77ºC) where MC changes to CC is, namely, transition zone (TZ). When a reservoir rock lies within the mechanical compaction zone, it is considered to be unconsolidated and vulnerable to subsidence. However, a small amount of cement at the grain contacts significantly increases the rock stiffness (Vernik and Nur, 1992; Dvorkin and Nur, 1996), and the rock becomes stiffer and changes the rock properties significantly. Therefore, it is crucial to know the regime (*i.e.* MC or CC) beause the reservoir rock might experience (maximum temperature and pressure).

This study identified the transition zone between mechanical and chemical compaction of three gas sands (Upper, Middle, and Lower gas sands) by tracking the changes in geophysical property in wire line logs from Well-2 of the X Gas Field (Figure 1). Moreover, quantitative cementation of primary reservoirs rocks was evaluated using the rock physic template.

Geological Setting

The Bengal Basin covers approximately 11,000 km^2, roughly half of which record deposition within offshore settings (Reimann, 1993). The basin contains approximately 20 km of Cenozoic siliciclastic sediments. The Ganges–Brahmaputra and associated or ancestral rivers have been transporting clastic sediments to the Bengal Basin (Uddin and Lundberg, 1999). The basin has two broad tectonic provinces: (1) stable shelf, where thin sedimentary successions overlie the rocks of the Indian craton in the northwestern part of Bangladesh and (2) thick basin fill that overlies the basement of undetermined origin in the south and east (Bakhtine, 1966; Khandoker, 1989). The

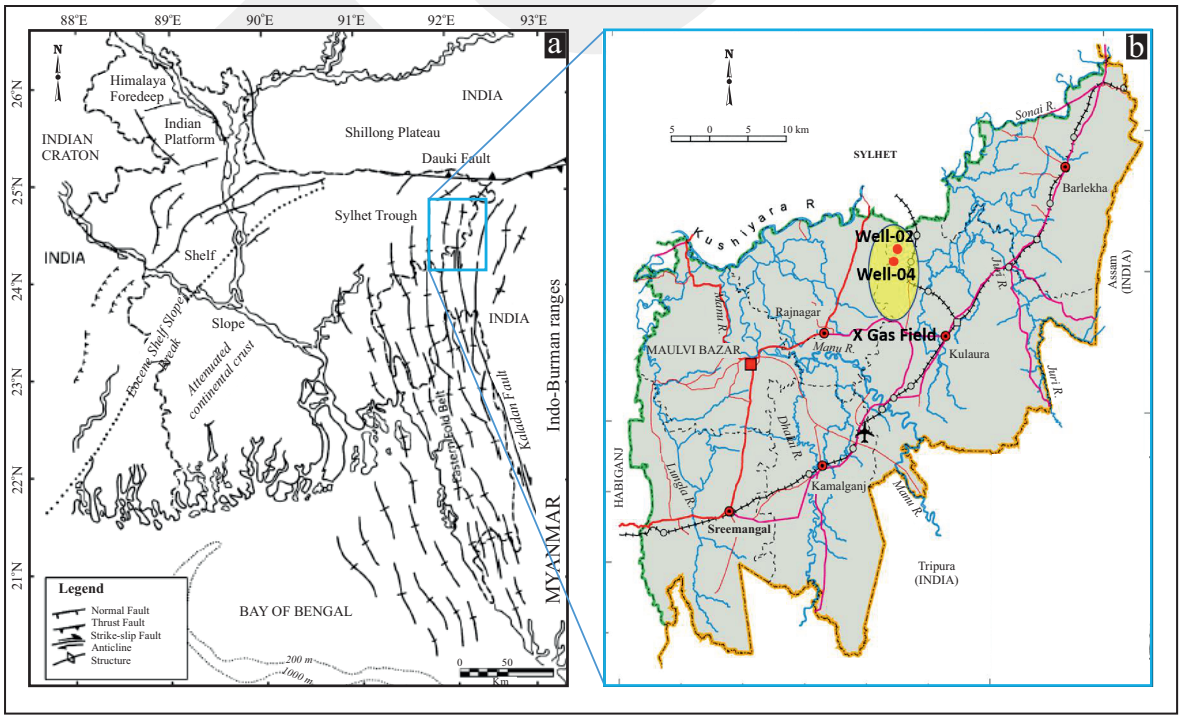

Figure 1. a) Map of the Bengal Basin shows the major structural elements (modified after Hossain, 2009), b) Location map of the studied X Gas Field (yellow circle) with the wells (modified after Banglapedia, 2020).

deeper part of the Bengal Basin is bounded by the hinge zone to the west and the fold belt to the east (Figure 1a). Compared to those in the fold belt area, strata in the deeper basin have experienced limited tectonic deformation. The Surma Basin is located in the northeastern part of the Bengal Basin, which was the main depocentre during Miocene. A series of N-S trending anticlinal folds are located in the eastern part of the Surma Basin, which possibly developed due to the Early to Middle Miocene collision between the Indian Plate and Burman Plate (Hiller and Elahi, 1988). The studied X gas field is one of this N-S trending anticline (Figure 1b).

The Surma Basin has been experiencing its evolutionary history when the Bengal Basin took the shape of a remnant ocean basin (Ingersoll *et al*., 1995) during Oligocene. By the Early Miocene, the Himalayas and Tibet started to uplift very rapidly, and a major upthrust movement of the Shillong Plateau along the Dauki Fault separated the Surma Basin from the stable shelf. Therefore, this basin became an active sediment depocentre. In the Eocene time, the paleo-depositional shelf was located on the Surma Basin when delta plain was farther north. The delta shelf edge shifted south in the Early Miocene, and the studied area became an upper shoreface to prodelta setting (Alam, 1995). The shelf edge continuously shifted southward, the Surma Basin became dominated by the intertidal to delta plain setting, which continued until Early Pliocene,

Table 1. Generalized Stratigraphic Succession in the Studied Area

Age	Formation	Depth (m)	Thickness (m)	LITHOLOGY
Late Pliocene	Dupi Tila	0 - 298	298	Mostly sandstone and minor clay. Sandstone is brown to light brown, coarse-grained, consolidated, moderately sorted, highly ferruginous, composed of quartz with few mica, quartzite pebbles, clay galls, and soft immature coal. Clay is dark grey, very soft, sticky, and soluble in water.
Middle Pliocene	Tipam	298 - 1150	852	Mostly sandstone and minor clay. Sandstone: light to off white, medium, poorly consolidated, ferruginous, mainly composed of quartz with few mica and dark colored minerals in place. Soft immature coal also present. Clay: grey to dark grey, soft to moderately hard and compact
Miocene	Upper Bokabil	1150 - 1466	316	Shale (UMS): grey to bluish grey, soft to moderately hard and compact and also laminated sandstone and shale alternation. Sandstoe: light to clear, medium to fine, moderately sorted, occasionally calcarious, composed of quarts with mica and variegated colored minarals.
	Middle Bokabil	1466 – 1766	300	Shale: grey to bluish, well laminated, silty, moderately hard, and compact. Mostly shale with minor sandstone.
	Lower Bokabil	1766 - 2236	470	Shale: grey to dark grey, hard and compact, well laminated, silty, and conchoidal fractured. Calcareous, composed mainly of quartz with mica and dark colored minerals.
Late Miocene	Upper Bhuban	2236 – 3150	930	Silty shale with fine-grained sanstone. Alternating grey to dark grey, well laminated shale and light grey sandstone, hard and well consolidated, clay pebbless also present' Alternation of grey to dark grey well well laminated shale and sandstone of light grey, hard and well consolidated clay pebbles also presents.
Middle Miocene	Middle Bhuban	3150 – 4290	1140	Grey to dark grey, hard and compact, poorly to well laminated shale with thin sand layers.
Early Miocene	Lower Bhuban	4290 – 4820	530	Grey to dark, hard and compact laminated shale. Light grey coarse to very fine non-calc sandstones.
Oligocene	Barail	4820 – 4977+	157+	Grey to dard grey hard and compact laminated shale. Light grey to grey fine to very fine, hard and consolidated, well sorted sub-angular sandstone. Very fine, heavy mineral such as tourmaline, garnet and laterite fragment also abundant inthe rock

* Note: Formation thickness and lithology are based on Well-2 and Well-3 from X Gas Field (BAPEX report, 2015). Coloured box indicates the gas bearing horizons in the Surma Group.

and the main Surma Group reservoir rock was deposited.

The Miocene Surma Group is divided into two units: 1) Bhuban and 2) Bokabil Formations (Holtrop and Keizer, 1970; Hiller and Elahi, 1984; Khan *et al*., 1988), both of which extend throughout the Bengal Basin. Johnson and Alam (1991) have interpreted the Lower Surma Group as prodelta to delta front deposits of a mud-rich delta system, while the upper Surma Group represents shallow marine deposits to a tide-dominated coastal setting within a cycle of a transgressive-regressive regime (Sultana and Alam, 2001). The thickness of this group varied significantly from 2,700 m to over 3,900 m (Parvin *et al*., 2019). The overall stratigraphy of the Surma Basin is given in Table 1.

The Surma Group reservoirs are divided into three main gas zones, namely upper gas sand (UGS), middle gas sand (MGS), and lower gas sand (LGS). Table 2 shows the top and base of the UGS, MGS, and LGS sands of Well-4 in the X gas field.

Table 2. Top and Base of Gas Sands of Well-4 in X Gas Field (Source: BAPEX report 2015)

Sand name	Top (m)	Base (m)
Upper Gas Sand	2020	2072
Middle Gas Sand	2522	2600
Lower Gas Sand	2649	2750

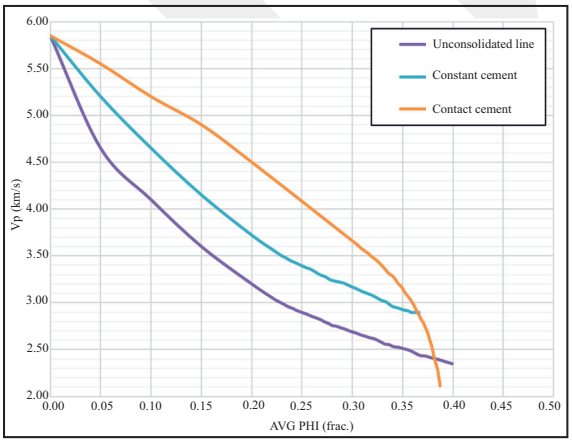

Figure 2. Vp versus porosity plot of rock physic template of unconsolidated (friable), constant, and contact cement models adapted from Avseth *et al*. (2005) and Rahman and Mondol (2017).

Methods and Analytical Techniques

The transition zone can be identified by the interpretation of the different geophysical logs. A sudden and distinct change in log properties can indicate changes from MC to CC. Moreover, the cement model can validate the depth range by evaluating cementation quantitively. A cement model is a rock-physical template where elastic properties (*i.e.* P wave velocity Vp, S wave velocity Vs, bulk density, *etc.*) of rock is plotted against porosity. In this study, Vp versus average porosity template is used to validate our transition zone analysis.

Wireline logs that are used in this study include Gamma-ray (GR), density (RHOB), neutron porosity (NPHI), and P-sonic log (DT). The density porosity was calculated from the bulk density log (RHOB) using the following equation:

$$\emptyset_{Density} = \frac{\rho_{matrix} - \rho_{bulk(log)}}{\rho_{matrix} - \rho_{fluid}} \quad \text{.....(1)}$$

where the matrix and the fluid density are assumed as quartz and brine density as 2.638 g/cc and 1.1 g/cc, respectively.

The neutron porosity log was corrected before being averaged using the following equation:

$$\emptyset_N = \emptyset_{neutron}\left[1 \times S_{XO} + HI_{gas} \times (1 - S_{XO})\right] \quad \text{.....(2)}$$

where:

$\emptyset_N$ is the neutron log porosity,

$\emptyset_{neutron}$ is the corrected neutron porosity,

S_{XO} is the saturation of mud filtrate, and

HI_{gas} is the hydrogen index of the gas of this formation.

The S_{XO} value of gas at 15-20% porosity is 0.85 (Asquith and Krygowski, 2004), which simplified the equation for porosity correction:

$$\emptyset_{neutron} = 1.11\emptyset_N \quad \text{.....(3)}$$

Finally, the average porosity was calculated using the following equation:

$$\emptyset_{Avg} = \sqrt{\frac{\emptyset^2_{density} + \emptyset^2_{neutron}}{2}} \quad \text{.....(4)}$$

The analysis was performed by plotting these logs in several ways. Plotting includes logs against depth, constructing cross plots, and plotting sonic and porosity logs with cement models.

Moreover, compressional velocity (Vp) is calculated from the P-sonic (DT) log using the following equation:

$$V_p = \frac{10^6}{DT}\ x\ 0.3048 \quad \text{.....(5)}$$

where *Vp* is in m/s, *DT* is in µs/ft.

The rock physic template used in this study is adapted from the previous study where the friable sand model is adapted from Rahman and Mondol (2017), and contact and constant cement (2%) models are adapted from Avseth *et al*. (2005). The constant cement model is a combination of the contact cement model and the friable cement model. The constant cement model assumes that the clastic rock has reduced porosity to a certain degree due to contact cement, whereas further porosity reduction is due to the noncontact-cemented particles located inside the pores (Grude *et al.,* 2015). Figure 2 has illustrated the cement models in which the upper and lower curves represent contact-cement (stiff) and friable (soft) sand model. Intermediate constant cement curve represents 2% contact-cemented line. These models were used to evaluate qualitative cementation within different reservoirs.

Result

Transition Zone Identification

Gamma-ray was used as a proxy for facies (sands or shales) as no core and cutting samples are available in this study. No distinct changes were observed in gamma-ray values except few local low and highs where the values range between 30 to 57 API (Figure 3a). There is a sharp increase in density, and a decrease in neutron porosity was identified at a depth of 2,576 m. The density above and below this depth shows the comparatively constant value with 2.2 and 2.65 g/cm^3, respectively (Figure 3b). A similar trend was also found in the neutron porosity plot where porosity ranges between 52% to 22% above and below the depth, respectively (Figure 3c).

Cross plot of NPHI versus RHOB of UGS, MGS, and LGS from Well-2 also reveals two distinct clusters with significantly different neutron and density values (Figure 4). The upper cluster

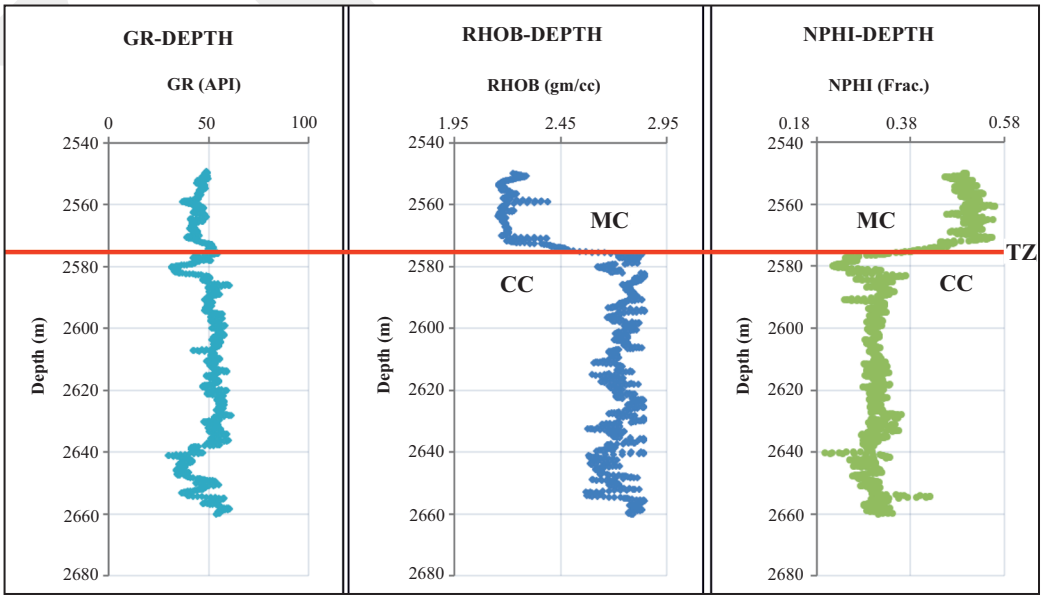

Figure 3. Plots of depth versus (a) gamma-ray, (b) density, and (c) neutron porosity logs from Well-2 showing that the transition zone is at 2,576 m between mechanical and chemical compaction in X Gas Field.

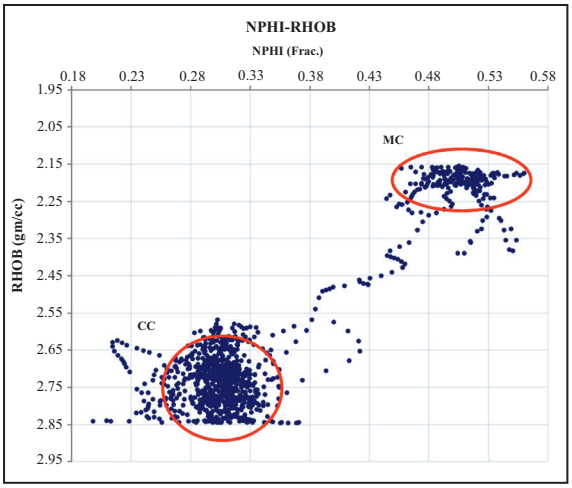

Figure 4. Cross plot of neutron porosity and density of UGS, MGS, and LGS from Well-2. The data clusters represent the variation of reservoir properties.

shows higher porosity and lower density than the lower cluster, where porosity decreases with increasing density significantly.

Rock Physical Analysis

For the quantitative analysis of this three-gas-sand, data from Well-4 was plotted with cement models. The average porosity was plotted against velocity to identify the quantitative cement percentage of different sands (Figure 5). The lower gas sand and lower part of the middle gas sand have higher sonic velocity and lower average

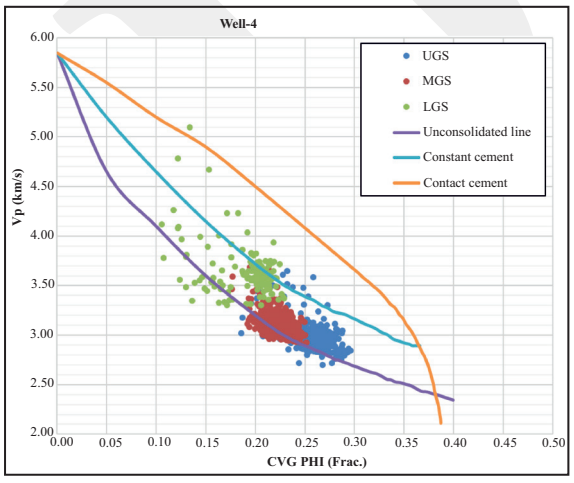

Figure 5. Cross plot of porosity versus velocity data points from Well-4 shows the variation of UGS, MGS, and LGS cement properties. The cement models are adapted from Avseth *et al.* (2005) and Rahman and Mondol (2017).

porosity compared to the upper gas sand and the upper part of the middle gas sand. The UGS followed the friable sand model, where porosity loses through compaction. Most of the MGS also followed the UGS trend. However, a few MGS and LGS points sharply increased the velocity with minimal porosity change and followed the 2% constant cement model. The data distribution illustrated the diagenetic differences within sandstones.

Discussion

Rock properties such as velocity, bulk density, and porosity continuously changes after deposition due to several compaction processes. Rock initially undergoes mechanical compaction (MC) up to a certain depth with a specific temperature (about 69 - 77ºC). This depth is called transition zone (TZ), as discussed earlier. In the MC regime, rocks are loose and uncemented and show higher porosity, lower density, and lower velocity than the rocks in chemical compaction zone. These changes are easily visible in wireline logs, and UGS and the upper part of MGS are located in mechanical compaction zone showing higher porosity and lower density and velocity (Figures 3 and 4).The transition zone starts at 2,576 m below which lower part of MGS and LGS has experienced chemical compaction zone.

As mechanical compaction is mainly controlled by the effective stress, it should be expected that the development of fractures and deformed grains in thin section of studied rock. The chemical compaction is associated with dissolution and precipitation of minerals within sedimentary rocks (reservoir rock), which are easily visible in thin section. Unfortunately, there was no core data for this study. However, two core analyses (2,420m and 3,420m) were adapted from Hossain (2009) who used core samples to identify over pressure and temperature at the Well-2 in the same X gas field. First core is located in identified mechanical compaction zone and second core

from chemical compaction zone. If two samples are compared, there is a significant decrease in porosity with increasing depth from 2,420 m to 3,420 m where porosity in the rocks from MC zone is significantly higher than the rocks in the CC zone (Figure 6).

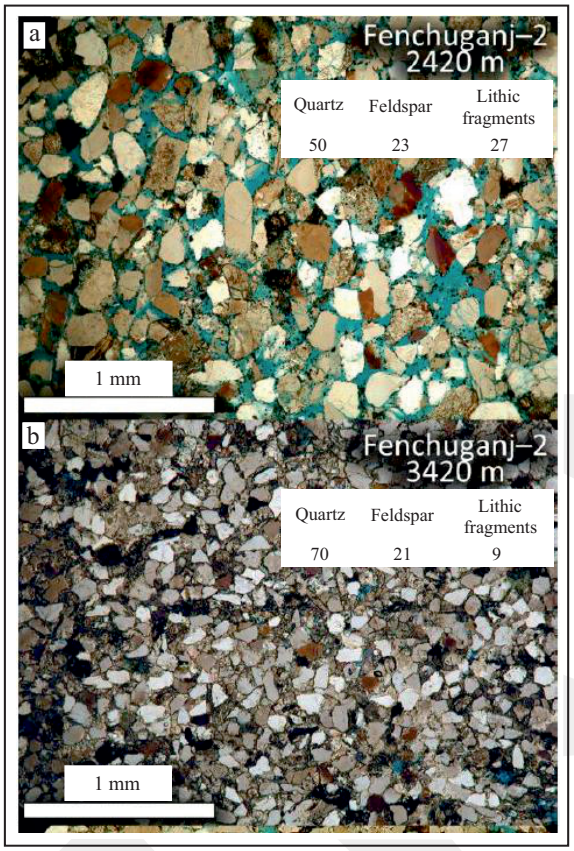

Figure 6. Photomicrographs of core samples of Well-02 shows the significant porosity differences at depth (a) 2,420 m and (b) 3,420 m. The XRD mineralogical data were also added for comparison (modified after Hossain, 2009).

The core sample analysis from 2,420 m shows the development of fractures in plagioclase feldspar along weak planes, which is probably because of mechanical compaction of the rock. The sample at 2,420 m depth also shows well-preserved primary interparticle porosity (blue stain) and grains are loosely packed which indicates that these rocks undergo mechanical compaction (Figure 7). The temperature in this zone is approximately 58ºC that is not high enough to initiate chemical compaction in this zone (Figure 8).

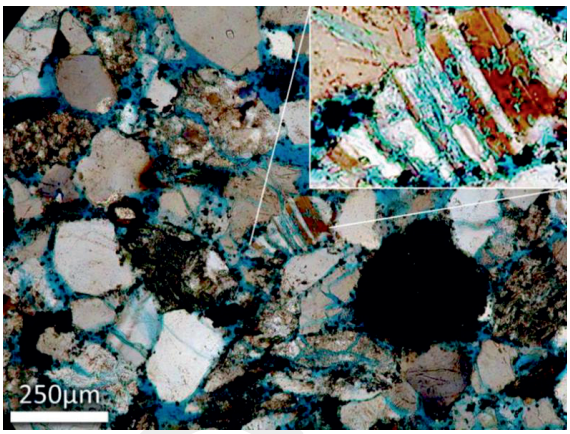

Figure 7. Photomicrograph shows development of fractures in plagioclase feldspar along weak planes (sandstone core sample from the Well–2 at 2,420 m depth).

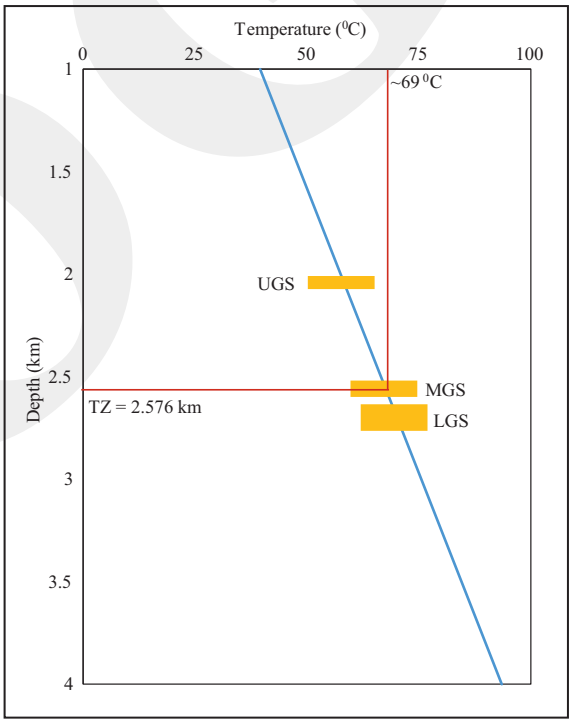

Figure 8. Temperature gradient calculated using Well-02 adapted from Hossain (2009).The yellow boxes show temperature of our studied reservoir rock.

The sample from 3,420 m depth shows a complete loss of primary interparticle porosity by matrix infilling (Figure 6b). Secondary porosity in sandstone develops through feldspar dissolution during deep burial (Hossain, 2009). The presence of corroded quartz grains, oversized pores, porosity channels between grains and cement, and partially dissolved rock fragments satisfies

the criteria for secondary porosity (Schmidt and MacDonald, 1976) which indicates that these rocks are located in a chemical compaction zone. Moreover, the quartz and lithic fragments percentage significantly change between the two depths. The quartz fraction increases by 20%, while lithic fragments decrease two-third (Figure 6). These lithic grains might be precipitated as quartz cementation, explaining the significant differences in mineralogy between them. In addition, the transition depth temperature in this zone is high enough (69º C) to initiate chemical compaction of the rock in this zone. Therefore, these analyses validate the findings of TZ depth and sandstones compaction history

As UGS and upper part of MGS are located above transition zone (TZ), they are loose, porous, and unstable. Below TZ, at the initial phase of chemical compaction, a small amount of cement at the grain contacts will significantly increase the stiffness (Vernik and Nur, 1992; Dvorkin and Nur, 1996) and cease the stress-dependent mechanical compaction even though the cement is relatively soft (Dvorkin *et al*., 1994). Cemented rock has a higher strength than an uncemented rock of the same porosity and mineralogy. Besides, the cemented rock permeability might be higher than that of uncemented rock at the same porosity. Because of loose pore-filling material or noncontact cement increases the specific area, it decreases permeability (Avseth *et al*., 2010). Therefore, during gas production, it should be kept in mind that these three reservoirs are vertically located in different compaction regimes, and the reservoir properties of these sands have variation. UGS and upper part of MGS are unconsolidated, which may lead to sending issues due to the overproduction. This also may trigger the overburden rock subsidence in the studied area as these rocks are loose and have no sufficient strength to hold overburden when gas is depleted. On the contrary, during any fluid injection for enhancing recovery in the lower part of MGS and LGS, the fluid type should carefully be chosen, because these zones are in the CC regime and have almost 2% cement. Improper fluids may react with the cement and seal the porosity instead of increasing them. However, reservoir quality depends on many other factors, *i.e.* temperature, pressure, *etc*. that need to be included during the reservoir management plan for sustainable development.

Conclusions

Identifying the cement model transition zone, analysis has revealed the qualitative and quantitative information about reservoir properties. The UGS and upper part of MGS are located in the mechanical compaction zone and vulnerable if overproduced. However, the lower part of MGS and entire LGS are experiencing chemical compaction. These reservoir rocks have sufficient strength, with almost 2% contact cement. However, their properties may degrade during improper chemical injections for enhanced recovery. Yet, very few works in rock physical have been done in Surma Basin. Therefore, it is recommended that every gas field should run this type of work for better reservoir management.

Acknowledgment

The authors are thankful to the Geology Department, the University of Dhaka, to carry out this research. The authors also appreciate BAPEX and Petrobangla for providing the data.

References

Alam M.M., 1993. Sedimentology and depositional environment of subsurface Neogene sediments in the Sylhet Trough, Bengal Basin: case study of the Fenchuganj and Beanibazar structures, northeastern Bangladesh. *Unpublished report*, Bangladesh Petroleum Institute, p.1 - 82.

Alam M.M., 1995. *Sedimentology and depositional environment of Bengal Basin subsurface Neogene succession based on detailed facies and electrofacies analysis: A case study*

of the Kailastila, Rashidpur, and Bakhrabad structures in northeastern Bangladesh. NORAD project BGD-023, Bangladesh Petroleum Institute, Dhaka,74 pp.

Asquith, G. and Krygowski, D., 2004. *Basic well log analysis*. AAPG methods in Exploration Series 16, 224pp.

Avseth, P., Mukerji, T., and Mavko, G., 2005. *Quantitative seismic interpretation: Applying rock physics tools to reduce interpretation risk*. Cambridge University Press, New York. DOI:10.1017/cbo9780511600074

Avseth, P., Mukerji, T., Mavko, G., and Dvorkin, J., 2010. Rock-physics diagnostics of depositional texture, diagenetic alterations and reservoir heterogeneity in high porosity siliciclastic sediments and rocks-A review of selected models and suggested work flows. *Geophysics,* 75, p.131-147. DOI:10.1190/1.3483770

Bakhtine, M.I., 1966, Major tectonic feature of Pakistan. Part-II. *Eastern Province: Science and Industry,* 4, p.89-100.

Banerji R.K., 1984. Post-Eocene biofacies, palaeoenvironments and palaeogeography of the Bengal Basin, India. *Palaeogeography, Paleoclimatology, Paleoecology,* 45, p.49-73. DOI: 10.1016/0031-0182(84)90109-3.

Dvorkin, J., Nolen-Hoeksema, R., and Nur, A., 1994. *The squirt-flow mechanism: macroscopic description. geophysics,* 59, p.428-438. DOI:10.1190/1.1443605

Dvorkin, J. and Nur, A., 1996. Elasticity of high-porosity sandstones: Theory for two North Sea data sets. *Geophysics,* 61(5), p.1363-1370. DOI:10.1190/1.1444059

Grude S., Dvorkin J., and Landrø M., 2015. Permeability variation with porosity, pore space geometry, and cement type: A case history from the Snøhvit field, the Barents Sea. *Geophysics,* 80 (1), p.D43-D49. DOI:10.1190/geo2014-0064.1

Hiller K. and Elahi M., 1988. Structural growth and hydrocarbon entrapment in the Surma Basin, Bangladesh. *In*: Wagner H.C., Wagner L.C., Wang F.F.H., and Wong F.L., (eds.), *Petroleum Resources of China and related subjects*, Huston, Texas. Circum-Pacific Council for Energy and Mineral Resource Earth Science Series, 10, p.657-669.

Holtrop J.F. and Keizer J., 1970. Some aspects of the stratigraphy and correlation of the Surma Basin wells, East Pakistan. *ECAFE Mineral Resource Development Service,* 36, p.143-154.

Hossain S.H., 2009. *Ovepressure in the eastern Bengal Basin, Bangladesh and its relation to compressional tectonics.* Master's thesis, Auburn University, Auburn, Alabama.

Ingersoll R.N., Graham S.A., and Dickinson W.R., 1995. *Remnant ocean Basin, Tectonics of sedimentary basin*. Blackwell, Oxford, p.363-391.

Khandoker, R.A., 1989. Development of major tectonic elements of the Bengal Basin: a plate tectonic appraisal. *Bangladesh Journal of Scientific Research,* 7, p.221-232.

Parvin A., Rahman M.J., and Woobaidullah, A.S.M., 2019. Petroleum prospect analysis and new gas horizon detection at Fenchuganj Gas field in the Surma Basin, Bangladesh: An application of the sequence stratigraphic concept. *Marine and Petroleum Geology,* 102, p.786-799. DOI: 10.1016/j.marpetgeo.2019.01.033.

Parvin A., Woobaidullah A.H.M., and Rahman M.J. 2019. Sequence stratigraphic analysis of the Surma Group in X Gas Field, Surma Basin, Bengal Delta. *Journal of Nepal Geological Society,* 58 (Sp. Issue), p.39-52. DOI: 10.3126/jngs.v58i0.24572.

Rahman J. and Mondol N. H., 2017. Lateral changes in reservoir properties of Stø Sandstone in the Snøhvit field, SW Barents Sea. *First Break*, 35 (7), p.35-40. DOI:10.3997/1365-2397.2017015

Reimann, K.U., 1993. *Geology of Bangladesh*: Berlin, Borntraeger.

Schmidt, V. and MacDonald, D.A., 1976. Texture and recognition of secondary porosity in sandstones: *Society of Economic Paleontologists and Mineralogists,* 26 *(Special Publication)*, p.209-225.

Sultana D.N. and Alam M.M., 2001. Facies analysis of the Neogene Surma Group succession in the subsurface of the Surma Basin, Bengal Basin, Bangladesh. *Bangladesh Geoscience Journal,* 6, p.53-74. DOI:10.1016/s0037-0738(02)00190-2

The National Encyclopedia of Bangladesh (Banglapedia), 2020. https://www.banglapedia.org/.

Uddin, A. and Lundberg, N., 1998a, Cenozoic history of the Himalayan-Bengal system; sand composition in the Bengal Basin, Bangladesh. *Geological Society of America, Bulletin,* 110, (4), p.497-511. DOI:10.1130/0016-7606(1998)110<0497:chothb>2.3.co;2

Vernik, L. and Nur, A., 1992. Ultrasonic velocity and anisotropy of hydrocarbon source-rocks. *Geophysics,* 57. DOI:10.1190/1.1443286